Chemical Engineering Science 152 (2016) 267–279

Contents lists available at ScienceDirect

Chemical Engineering Science

journal homepage: www.elsevier.com/locate/ces

Experimental study on drag reduction performance of surfactant flow in longitudinal grooved channels

Chonghai Huang [a], Dongjie Liu [a], Jinjia Wei [a,b,*]

[a] State Key Laboratory of Multiphase Flow in Power Engineering, Xi'an Jiaotong University, No. 28, Xianning West Road, Xi'an 710049, China
[b] School of Chemical Engineering and Technology, Xi'an Jiaotong University, No. 28, Xianning West Road, Xi'an 710049, China

HIGHLIGHTS

- Collaborative effect of surfactant solution and longitudinal grooves was explored.
- Drag reduction mechanisms of surfactant and grooves are complementary.
- Drag reduction effect of surfactant solution is enhanced by longitudinal grooves.
- Drag reduction range of longitudinal grooves widens in surfactant solution.
- Drag-reduction enhancement mechanisms of surfactant by grooves are analyzed.

ARTICLE INFO

Article history:
Received 1 April 2016
Received in revised form
17 May 2016
Accepted 4 June 2016
Available online 15 June 2016

Keywords:
Drag reduction
Surfactant
Longitudinal microgroove
Collaborative
Enhancement

ABSTRACT

Drag-reducing surfactant solution can provide a large-eddy environment for longitudinal microgrooves and may realize the complementarity between their drag-reduction mechanisms. In this work, the collaborative drag reduction performance of surfactant solution and longitudinal microgrooves was experimentally studied to verify the speculation about their complementary possibility. The mixture aqueous solution of cationic surfactant (cetyltrimethyl ammonium chloride) and counterion salt (NaSal) was tested in the smooth and two longitudinal microgroove channels respectively at the mass concentrations of 0.16–0.47 mmol/L. It was found that the drag reduction performance of surfactant solution was enhanced by the longitudinal microgrooves. The drag-reduction mechanisms of microgrooves in water and surfactant solution were illustrated by the competition between the “peak effect” and the “restriction effect” of microgroove. Moreover, the “second peak effect” was proposed to explain the drag-reduction enhancement mechanisms for surfactant flow in microgroove channels. The groove with a larger size and roughness which might increase the drag in water could still enhance the drag reduction effectiveness of surfactant flow, and had a lower critical temperature and critical Reynolds number in surfactant solution, indicating a promising application in the heat transfer and drag reduction field. Moreover, the results of particle image velocimetry of smooth channel indirectly verified that the drag-reducing mechanism of microgroove was related to the turbulent vortex scale and the restriction effect on near-wall vortices.

1. Introduction

Drag reduction effectiveness of 60–80% can be achieved by adding small amounts of surfactant to pipe or channel flow (Li et al., 2004). Compared with polymers, surfactants are more advantageous for the application in the closed cycle pipeline due to its reversible mechanical degradation characteristic (Bewersdorff and Ohlendorf, 1988; Ohlendorf et al., 1986). Therefore, it has been widely studied and concerned by scholars. One successful application of surfactant was in hydronic heating systems in a Czech city, in which drag reduction effectiveness of up to 70% was obtained by appropriate concentration of fresh drag-reducing additives (Myska and Mik, 2003).

After years of research, although the understanding of the drag reduction mechanism of surfactant is still imperfect, some physical insights have been revealed. Debye and Anacker (1951) reported that micelle structures of surfactant transformed from spherical to rod-like, wormlike or reticular micelles with increasing concentration. Rehage et al. (1985) found the shear-thickening and

* Corresponding author at: State Key Laboratory of Multiphase Flow in Power Engineering, Xi'an Jiaotong University, No. 28, Xianning West Road, Xi'an 710049, China.
E-mail address: jjwei@mail.xjtu.edu.cn (J. Wei).

http://dx.doi.org/10.1016/j.ces.2016.06.009
0009-2509/© 2016 Elsevier Ltd. All rights reserved.

shear-thinning phenomena in surfactant solution, and proposed that the shear-thickening transition was an important factor for the drag reduction of surfactant. Thereafter, Wei et al. (2009) investigated the turbulent structures of surfactant by particle image velocimetry (PIV) technique and reported that the formation of small-scale turbulent vortices was inhibited by addition of surfactants, resulting in a large-eddy environment which provided an excellent condition for other drag reduction methods related to the scale of turbulent vortex. Moreover, Mizunuma et al. (2010) and Ma et al. (2011) both found the mutual inhibition phenomenon between drag reduction and heat transfer performance of surfactant, limiting the application of surfactants in the field of heat transfer.

Compared with surfactant which reduces drag by altering the fluid composition and affecting the flow, another drag-reduction method uses passive devices which directly affect the flow without altering the fluid composition (Moaven et al., 2013). The longitudinal microgroove is one of them. Most of the investigations of longitudinal microgroove were carried out in Newtonian fluid and drag reduction occurred only in the low Reynolds numbers (Walsh, 1980, 1982; Walsh and Lindemann, 1984). Bechert et al. (1986), Choi (1990) and Koury and Virk (1995) suggested from the investigations of longitudinal microgrooves with different shapes that the longitudinal microgrooves could inhibit the formation of low-speed streaks and restrict the spanwise motions of near-wall streamwise vortices, resulting in decreasing turbulent kinetic energy exchange and surface friction. Moreover, Zhang et al. (2011) revealed a larger shear stress near the grooved tip. Chamorro et al. (2013) pointed out that the drag reduction performance of microgroove was related to its size, implying that the scale of near-wall vortices had a significant influence on the drag reduction effect of microgroove.

By analyzing the existing research of surfactants and longitudinal microgrooves, a complementarity between their drag-reduction mechanisms could be speculated. Therefore, when the longitudinal microgrooves are applied in surfactant solutions, the drag reduction of longitudinal microgroove should be occurred at a higher Reynolds number which is much closer to the actual industrial situation, and the drag reduction performance of surfactant could be further enhanced by microgroove through utilizing the large-eddy environment in surfactant solution. Moreover, the drag-reduction size of longitudinal microgroove might be enlarged due to the increasing scale of vortex in surfactant solutions. Therefore, the coupling study between them is beneficial to improve their application values in the practical industry. However, there is little information available on their coupling study. Thus, the purpose of this study is to verify the speculation mentioned above about the complementarity of drag-reduction mechanisms between surfactant and longitudinal microgroove.

2. Experimental

2.1. Test facility

The experiments were performed on a closed loop shown schematically in Fig. 1. The system consisted of a storage tank, a stainless steel centrifugal pump, a settling chamber, a two-dimensional (2D) channel, a diffuser and other necessary elements. A 6 kW heater installed in the storage tank was used to control the fluid temperatures with an accuracy of ± 0.1 K. The low flow rate (0.7–3 m^3/h) and high flow rate (>3 m^3/h) were measured respectively by two parallel electromagnetic flowmeters (L-mag B Type, Xi'an Xu Sheng Instrument Co., Ltd., measuring accuracy of 0.001 m^3/h and 0.01 m^3/h respectively). The flow rates were adjusted by the motor frequency of a stainless steel centrifugal pump. The pressure drop of the test channel was measured by two pressure taps with a distance of 1.1 m (L), using a differential pressure transmitter (Transmitters with Capacitive Sensor, Chang Hui Automation System Co. Ltd., measuring range of 0–10 kPa and measuring accuracy of 5 Pa).

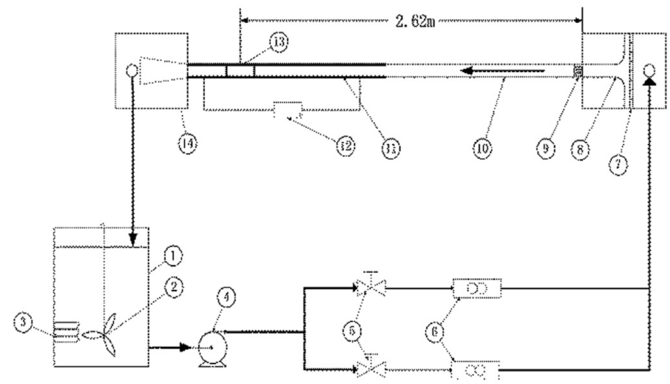

Fig. 1. Schematic of experimental system. (1) Storage tank; (2) stirrer; (3) heater; (4) stainless steel centrifugal pump; (5) valve; (6) electromagnetic flowmeter; (7) filter; (8) contraction; (9) honeycomb; (10) 2D channel; (11) test section; (12) differential pressure transmitter; (13) window for PIV; (14) diffuser.

The 2D channel of 10 mm height (H), 125 mm width (W) and 3 m length consisted of a fully developed section and a test section. Each section was 1.5 m. The aspect ratio of the 2D channel was more than 7 to insure a two-dimensional flow in the center of the spanwise distance. The fully developed section was long enough to ensure that the fluid in the test section developed a full turbulence. The test section could be replaced with the smooth channel or the grooved channel. For the longitudinal grooved channel, the reduction of the flow redevelopment length of surfactant solution at the leading edge of the longitudinal grooved channel could be achieved by ensuring that the flow area of grooved channel approximately equals to that of the fully developed section. Moreover, a distance of 25H is reserved from the leading edge of grooved channel to the pressure tap for fully redevelopment. The cross-section of the 2D channel is shown schematically in Fig. 2. It can be seen that the height of the channel was determined by two bulges of $H'=10$ mm for smooth channel, $H'=9.6$ mm for G1 channel and $H'=9.8$ mm for G2 channel to ensure the mean height of $H=10$ mm for each channel, since the half of the height of the groove was used as the datum plane (the height of groove is 0.4 mm for G1 and 0.2 mm for G2 in the present experiment). In this way, the flow area of grooved channel could approximately equal to that of smooth channel. Moreover, in order to further ensure the size of channel, a micrometer is also used to measure the height of channel after assembly for each channel. The PIV measurement position was 2.62 m ($=262H$) downstream from the inlet of 2D channel.

2.2. PIV measurement

The PIV system consisted of a double-pulsed laser, laser sheet optics, high-speed camera (SpeedSense Model 9040), timing circuit (Model 80N77), time trigger, image-processing software

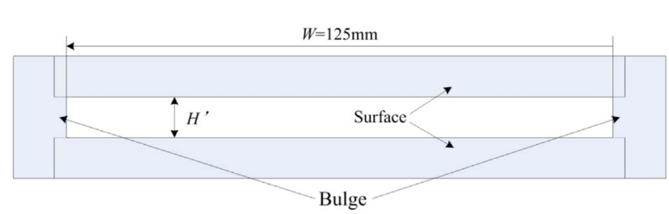

Fig. 2. Schematic diagram of cross section of the channel.